Carbohydrate Polymers 114 (2014) 57–64

Contents lists available at ScienceDirect

Carbohydrate Polymers

journal homepage: www.elsevier.com/locate/carbpol

Electrolyte effect on gelation behavior of oppositely charged nanocrystalline cellulose and polyelectrolyte

Ang Lu[a,b], Yongbo Song[c], Yaman Boluk[a,d,*]

[a] Department of Civil and Environmental Engineering, University of Alberta, Edmonton, AB, T6G 2G2, Canada
[b] Department of Chemistry, Wuhan University, Wuhan 430072, China
[c] Department of Agricultural, University of Alberta, Edmonton, AB, Canada T6G 2P5
[d] National Institute for Nanotechnology, National Research Council of Canada, Edmonton, AB, Canada T6G 2M9

ARTICLE INFO

Article history:
Received 11 June 2014
Received in revised form 16 July 2014
Accepted 19 July 2014
Available online 27 July 2014

Keywords:
Nanocrystalline cellulose
Gelation
Opposite charge
Electrolyte

ABSTRACT

The electrolyte (NaCl) influences on the sol–gel transition of the complex solution composed of oppositely charged nanocrystalline cellulose (NCC) and polyelectrolyte (quaternized hydroxyethylcellulose ethoxylate, QHEC) were investigated by the rheological means in the present paper. Winter and Chambon theory was applicable to describe the sol–gel transition, and the critical gel points have been successfully determined. When increasing the NaCl concentration, more NCC were needed to form a critical gel due to the screening of the electrostatic interaction, and the larger loss tangent and relaxation exponent (n) values at the gel point demonstrated a less elastic nature of the complex solution with more NaCl. The results indicated the gel network was composed of entanglements and association of QHEC (as polymer network), as well as the electrostatic adsorption interaction between QHEC chains and NCC rods (as cross-linking). With the addition of NaCl, the screening effect led to the enhancement of the entanglements and weakening of the electrostatic adsorption, however, the gel strength decreased with increasing the NaCl amount, suggesting the electrostatic adsorption interaction played a more dominant role than the entanglements when the gel was formed. Moreover, the exponents of the scaling law $\eta_0 \propto \varepsilon^{-\gamma}$ and $G_e \propto \varepsilon^z$ of the QHEC/NCC/NaCl solution revealed that the scaling law $n = z/(z+\gamma)$ between n, γ, and z was only feasible at the highest NaCl concentration, as a result of that the intermolecular electrostatic interaction was completely screened, indicating the scaling law was only feasible when intermolecular interaction was small enough to be neglected.

1. Introduction

Colloidal suspensions has been extensively recruited in a wide range of applications, such as paints (Farrokhpay, 2009; McGrath, Bock, Cathcart, & Lyon, 2007), coatings (Kleinert, Kim, & Velev, 2010), pharmaceutical formulations (Qi et al., 2011; Zuzzi, Cametti, Onori, Sennato, & Tacchi, 2009), food (Canales, Hidalgo, Risso, & Alvarez, 2010) and so forth (Leunissen et al., 2005; Lee, Gradon, Janeczko, Iskandar, & Okuyama, 2010; Sabourin, Dabbs, Yetter, Dryer, & Aksay, 2009; Huang et al., 2012; Chen et al., 2011; Liu, Zhong, Chang, Li, & Wu, 2010; Liu et al., 2014). The gelation phenomenon in colloidal suspensions can be described as the aggregation of attractive particles into a network structure with mechanical stability (Whitmer & Luijten, 2011), which is relevant in a broad range of settings, including biological systems and industrial applications (Lee, Chan, Bevan, Lewis, & Braun, 2004; Martinez et al., 2005), such as food products (Allen, Murray, & Dickinson, 2008), cosmetics (Gallegos & Franco, 1999), high-performance coatings and so forth (Larson, 1999; Russel, Saville, & Schowalter, 1989). The rheological properties of colloidal gels attribute to the micromechanical properties of the gel backbone, dominated by nano-scale particle interactions (Pantina & Furst, 2004; Liu, Chen, Yue, Chen, & Wu, 2011).

Polyelectrolyte plays an important role in diverse fields ranging from materials science and colloids to biophysics (Carrillo & Dobrynin, 2011), and complex systems composed of oppositely charged colloids and polyelectrolytes exhibit complicated self-aggregation behaviors, because of the electrostatic interactions (Pickrahn, Rajaram, & Mohraz, 2010; Hoffmann et al., 2011; Kumar, Dubin, Hernon, Li, & Jaeger, 2007). The structures formed by oppositely charged macroions and polyelectrolytes vary in a large dimension range, with respect to the detailed structural organization, and such mixtures have great potentials (Wang & Roman,

* Corresponding author at: National Research Council of Canada, National Institute for Nanotechnology, Edmonton, AB, Canada T6G 2M9. Tel.: +1 780 492 6295.
E-mail address: yaman.boluk@ualberta.ca (Y. Boluk).

http://dx.doi.org/10.1016/j.carbpol.2014.07.040
0144-8617/

2011a,b; Sivakumar et al., 2009; Yap, Quinn, Ng, Cho, & Caruso, 2005; Ye, Tong, & Fetters, 1997). Important aspects pertaining to the nature of the electrostatic interaction and its relations to phase behavior and phase structure in these systems are beginning to be understood (Hansson, 2006), and an important undertaking in this area should be to quantify the role of electrostatic interactions in complex formation between oppositely charged colloids and polyelectrolyte. More generally, the role of electrostatic interactions in the self-assembly or self-organization in charged macromolecular systems is still lacking of detailed investigation.

Addition of electrolyte to an oppositely charged colloids/polyelectrolyte complex system leads to screening of the electrostatic interactions between ionized groups, reducing the polyelectrolyte effect and affecting the conformation of polymers (Dobrynin & Rubinstein, 2005; Colby, 2010), resulting in a huge variance to the charged colloid/polyelectrolyte system and tunable rheological behavior of the complex system (Brotherson, Bottomley, Ludovice, & Deng, 2008), which is important and can be very useful in material science and technology. In the present paper, the effect of a monovalent electrolyte (NaCl) on the gelation behavior as well as the rheological properties and scaling law application of a mixture, composed of oppositely charged nanocrystalline cellulose (NCC) colloid suspension and polyelectrolyte (quaternized hydroxyethylcellulose ethoxylate, QHEC) aqueous solution, was detailed investigated. The microstructure and dynamics at the gel point have also been revealed. We hope to provide useful fundamental information about the electrolyte influences on the interactions between oppositely charged colloids and polyelectrolyte, as well as the sol–gel transition behaviors, to promote the advance and development of colloids/polymer composite materials.

2. Experimental

2.1. Materials

Lyophilized nanocrystalline cellulose (NCC) particles were supplied by Alberta Innovates Technology Futures (Edmonton, Alberta, Canada). Specifically, NCC particle sample was prepared by acid hydrolysis of commercial dissolved kraft softwood pulp. Pulp was hydrolyzed with 64% sulfuric acid using a 1:8 weight ratio at 50 °C for 40 min and then diluted with de-ionized water to quench the reaction. The suspension was then centrifuged at 6000 rpm for 10 min, neutralized with Na_2CO_3 and dialyzed to remove the salts. Finally, the suspension was further dispersed in an ultrasonic bath to achieve 1–2% concentration stable colloidal suspension. NCC particles were obtained in powder form by lyophilizing the suspensions. Detailed preparation method was discussed elsewhere (Bondeson, Mathew, & Oksman, 2006; Boluk, Zhao, & Incani, 2012), and NCC particles used in the present paper exhibited average length of 87 nm, average diameter of 16 nm, average aspect ratio of ~5.4 and ζ-potential of −58.2 mV (Lu, Hemraz, Khalili, & Boluk, 2014a). NaCl was purchased from Fisher Scientific (Fair Lawn, NJ). Cationic polyelectrolyte quaternized hydroxyethylcellulose ethoxylate (QHEC) was purchased from Sigma-Aldrich (St. Louis, MO, USA), with a molecular weight between 400,000 and 500,000, cationic substitution of about 5 wt% and charge density of 1.2 mEq g^{-1} (Dalvi & Dave, 2009; Junka, Sundman, Salmi, Österberg, & Laine, 2014; Frenzel, Swaboda, Petzold, Emmler, & Simon, 2011; Regismond, Heng, Goddard, & Winnik, 1999). All materials were used without further purification.

2.2. Samples preparation

Water was purified by the Millipore Milli-Q system. QHEC was dissolved in NaCl aqueous solution to form QHEC/NaCl aqueous solutions, and NCC was dispersed in water to form NCC aqueous suspensions. QHEC/NCC/NaCl mixture samples were prepared by mixing appropriate quantities of aqueous stock solutions of QHEC/NaCl solutions and NCC suspensions. The samples were stirred and left for equilibration at room temperature for 3 day. In the QHEC/NCC/NaCl complex solution, QHEC concentrations (c_{QHEC}) were constant to be 1.5 wt%, due to a proper viscosity and sensitive response to the introduction of NaCl (which will be demonstrated later), while the NaCl concentration (c_{NaCl}) was various, and at each NaCl concentration, NCC concentration (c_{NCC}) was changed in the range from 0 to 0.39 wt% (during c_{NCC} range, the QHEC/NCC solution undergoes phase transition from liquid to gel, which was ready for investigation), which was influenced by the different amount of NaCl.

The phase behavior was determined by visual inspection. All the tested samples displayed one homogeneous phase.

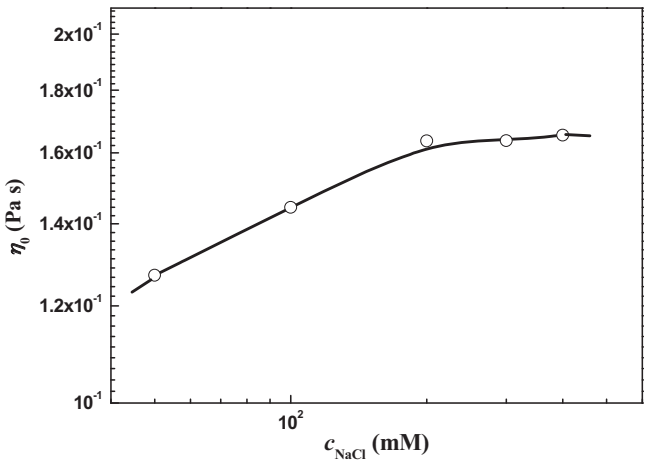

Fig. 1. Zero-shear viscosity (η_0) of 1.5 wt% QHEC in NaCl solution as a function of NaCl concentration (c_{NaCl}).

2.3. Characterization

The dynamic rheological measurement of the QHEC/NCC/NaCl complex solution was carried out on an AR-G2 rheometer (TA Instruments, USA). Cone and plate (2° nominal angle) geometry was used to measure the dynamic oscillatory parameters. The strain used for the linear viscoelastic region was determined by performing amplitude sweep experiments at a frequency of 1 rad s^{-1}. Temperature control was established with a ThermoCube 200/300/400 (Solid State Cooling Systems Co., USA) kept within ±0.05 °C of the desired temperature. In order to reduce the testing experimental error, all experiments were repeated twice.

3. Results and discussion

Fig. 1 shows the zero-shear viscosity (η_0) of 1.5 wt% QHEC in NaCl aqueous solution as a function of NaCl concentration (c_{NaCl}). The η_0 values increased in the beginning, followed by a plateau when c_{NaCl} was higher than 200 mM. QHEC molecular chain was electrostatically repulsed by each other in the aqueous solution as a result of the positive charge along the chains. When salt added, the electrostatic interaction between QHEC chains was partially screened, and stronger entanglement and association of the chains occurred, leading to a denser network. And the increasing viscosity was due to the denser 3-D network. When c_{NaCl} was higher than 200 mM, the electrostatic interaction was completely screened by NaCl stoichiometrically and QHEC behaved as uncharged macromolecules in the solution, therefore, further increasing c_{NaCl} made

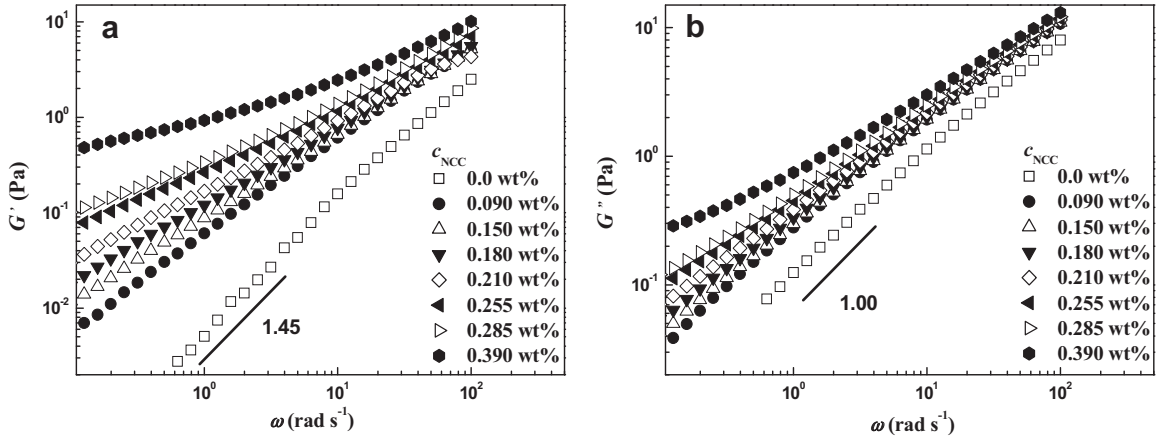

Fig. 2. Storage modulus $G'(\omega)$ (a) and loss modulus $G''(\omega)$ (b) of the 1.5 wt% QHEC with various NCC concentrations in 100 mM NaCl solution as a function of angular frequency ω at 25 °C. Values represent the slope of the line.

no influences to the chain conformation and the viscosity stayed constant. According to the result from Fig. 1, the c_{NaCl} used in the present paper was 50, 100 and 200 mM, to reach different screening of the electrostatic interactions in the complex system.

Winter and Chambon's theory (Chambon & Winter, 1985, 1987; Winter & Chambon, 1986) was used to determine the critical gel point of QHEC/NCC/NaCl instead of the traditional method, in which the crossover of storage modulus (G') and loss modulus (G'') was regarded as the gel point (Tung & Dynes, 1982). Moreover, the frequency independence of the loss tangent value ($\tan\delta = G''/G'$) in the vicinity of the gel point has been widely examined for gels and has been employed to determine the gel point (Lue & Zhang, 2008; Shi et al., 2012; Song, Niu, Wang, & Zhang, 2011; Madbouly, Xia, & Kessler, 2012; Wang, Lue, & Zhang, 2009). Fig. 2 shows the $G'(\omega)$ (a) and $G''(\omega)$ (b) of the 1.5 wt% QHEC with various NCC concentrations (c_{NCC}) in 100 mM NaCl solution at 25 °C. Both $G'(\omega)$ and $G''(\omega)$ curves increased with an increase of c_{NCC} and the curves became flat with smaller slope versus frequency, indicating a mutative network formation. It was noted that the dynamic mechanical behavior of the QHEC/NCC/NaCl solution followed liquid-like terminal behavior at very low c_{NCC}, whereas deviations became more obvious at higher c_{NCC}. When the c_{NCC} was 0, the low frequency slopes of $G'(\omega)$ and $G''(\omega)$ curves have been calculated to be

$$G'(\omega) \propto \omega^{1.45} \quad G'(\omega) \propto \omega^{1.00} \quad (\omega \to 0) \tag{1}$$

While at the highest c_{NCC}, the plateau of $G'(\omega)$ at low frequency was the sign of the formation of a gel network, according to the method by Nijenhuis and Winter (1989). Therefore, it was reasonable to consider that the sol–gel transition has occurred in the range of c_{NCC} variation. The QHEC/NCC/NaCl solution at other NaCl concentrations exhibited similar behaviors, so that they were not shown here.

Fig. 3 shows the $\tan\delta$ plots of 1.5 wt% QHEC solutions with various NCC concentrations in 50, 100 and 200 mM NaCl aqueous solutions, respectively. It is noted that all the $\tan\delta$ value decreased with an increase of c_{NCC}, indicating the system became less viscous. When the c_{NaCl} was 50 mM, the $\tan\delta$ curve of the QHEC/NCC/NaCl solution composed of 1.5 wt% QHEC and 0.1605 wt% NCC reached a plateau value close to 2.70, exhibiting a frequency-independence behavior in the range from 0.1 to 20 rad s^{-1}. Moreover, when c_{NaCl} were 100 and 200 mM, two $\tan\delta$ curves exhibiting similar plateau behaviors with different c_{NCC} was observed, showing the plateau $\tan\delta$ values of 2.77 and 2.92, respectively, and the data were summarized in Table 1. Therefore, at each c_{NaCl} (50, 100 and 200 mM), a $\tan\delta$ curve obeyed Winter and Chambon theory was observed, indicating the gel point induced by adding different amount of NCC (0.1605, 0.189 and 0.222 wt%). The relevant c_{NCC} were then regarded as the gel concentration ($c_{g,NCC}$). n value at the gel point can be obtained by $\tan\delta$ value at each frequency-independent range.

$$\frac{G''(\omega)}{G'(\omega)} = \tan\delta = \tan\left(\frac{n\pi}{2}\right) \tag{2}$$

which were also summarized in Table 1. The results suggested the sol–gel transition of complex solution composed of QHEC, NCC and NaCl could be well described by Winter and Chambon theory. The approximate value of the zero-shear viscosity (η_0) could be obtained from the complex viscosity η^* at $\omega \to 0$, therefore, the value of η^* at the lowest tested frequency was defined as η_0 (Li, Uchida, & Aoki, 1997). Fig. 4 shows η_0 obtained from η^* as a function of c_{NCC} at 1.5 wt% QHEC in 50, 100 and 200 mM NaCl solutions. The η_0 versus c_{NCC} curves obtained break points, and interestingly the c_{NCC} at the breaks were in accordance with the $c_{g,NCC}$ from Fig. 3, indicating that η_0 tended to diverge near its gel point.

Table 1 shows the experimental values of the QHEC/NCC/NaCl solution. Obviously, the $c_{g,NCC}$ values increased with increasing c_{NaCl} with a constant c_{QHEC}, indicating that more NCC were needed to form gels at relatively higher c_{NaCl}, as a result of the screening of electrostatic interactions. On the other hand, the $\tan\delta$ value increased with increasing c_{NaCl}, indicating the complex system became less elastic. It is well known that the shear relaxation modulus $G(t)$ can be predicted by a power law relaxation at the critical gel point by Izuka and Winter (1992):

$$G(t) = S_g \times t^{-n} \tag{3}$$

where S_g is the gel strength and has an unusual dimension of Pa s^n, and n is the relaxation exponent that determines the stress relaxation rate at the gel point, which can be calculated by Eq. (2). To express S_g by Eq. (3), a similar expression can be applied to $G'(\omega)$ and $G''(\omega)$ at the gel point as

$$G'(\omega) = \frac{G''(\omega)}{\tan\delta} = S_g\,\omega^n\,\Gamma(1-n)\cos\left(\frac{n\pi}{2}\right) \tag{4}$$

with $\Gamma(1-n)$ is the Γ function.

Generally, the n value was relevant to the physically fractal dimension, and reflected the degree of compactness of the network, and the lower values of n implied a more highly elastic gel (Gao & Nishinari, 2004; Nordby, Kjøniksen, Nyström, & Roots, 2003; Kjøniksen, Hiorth, Roots, & Nysrtom, 2003). The larger $\tan\delta$ and n values at higher c_{NaCl} in Table 1 suggested a less elastic, as a result of the screening. Moreover, the physical nature of a gelling system at the gel point can also be described by the S_g. For chemical

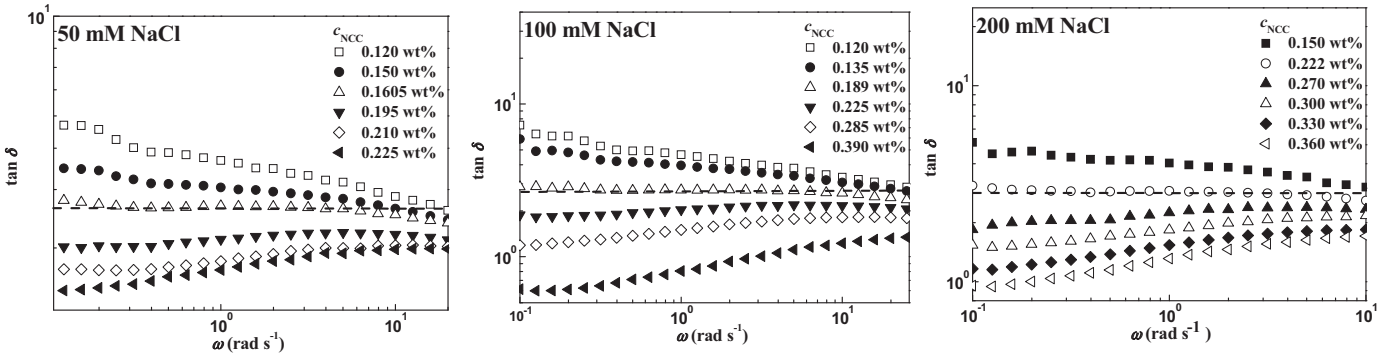

Fig. 3. tan δ plots of 1.5 wt% QHEC solutions with various NCC concentrations in 50, 100 and 200 mM NaCl aqueous solutions, respectively.

Table 1
The experimental values of critical gel concentration $c_{g,NCC}$, tan δ, relaxation exponent n (from both tan δ and scaling law) and gel strength S_g of the QHEC/NCC/NaCl solution.

c_{NaCl} (mM)	c_{QHEC} (wt%)	$c_{g,NCC}$ (wt%)	tan δ	n from tan δ	S_g (Pa s^n)	n From scaling law
0	1.5	0.159	2.66	0.771	0.0924	0.627 (Lu, Wang, and Boluk (2014)
50	1.5	0.1605	2.70	0.774	0.0886	0.696
100	1.5	0.189	2.77	0.780	0.0872	0.752
200	1.5	0.222	2.92	0.790	0.0869	0.799

gels, the S_g rose while n decreased, as a result of the increase of the cross-linking density, suggesting that S_g was related to the physical strength of the gel network at the gel point (Kjøniksen & Nystrom, 1996). Fig. 5 shows the plots of G' and $G''/\tan\delta$ against the c_{NCC} of 1.5 wt% QHEC in 100 mM NaCl solution. The G' and $G''/\tan\delta$ curves of different frequency groups exhibited ascending functions with increasing c_{NCC}. Interestingly, the intersects at the gel point lied at the same concentration ($c_{g,NCC}$ = 0.189 wt%), which was consistent to the results obtained according to Winter and Chambon theory. The plots of G' and $G''/\tan\delta$ against c_{NCC} at the other c_{NaCl} displayed similar behaviors, thus they were not shown here. By using any value of G' at the critical gel point according to Eq. (4), the S_g value were calculated. The curve of S_g versus c_{NaCl} is plotted in Fig. 6. S_g decreased in the beginning followed by a plateau, suggesting the physical strength of the critical gel was decreased with adding NaCl, which was in accordance with the conclusions drawn from tan δ and n. The plateau was caused by the completely screening of the electrostatic interactions, similar with the result from Fig. 1. In the QHEC/NCC system, the gelation was induced by both electrostatic adsorption between QHEC and NCC as cross-linking, as well as the entanglements of QHEC polymers as network (Lu, Wang, & Boluk, 2014b). When NaCl was added, the electrostatic adsorption was weakened and the so-called cross-linking were reduced, therefore, more entanglements were needed to reach the gel network, leading to larger $c_{g,NCC}$ at higher c_{NaCl}. On the other hand, however, the screening also led to denser QHEC networks since the QHEC chains were easier to contact with each other. Therefore, smaller S_g suggested that the electrostatic adsorption between QHEC and NCC exhibited more dominant contribution than the QHEC entanglements to gel formation.

Furthermore, the effect of electrostatic interaction screening were demonstrated by Fig. 7, which shows contrary η^* behaviors of 1.5 wt% QHEC (a) and 1.5 wt% QHEC/0.21 wt% NCC (b) with NaCl addition. In Fig. 7(a), only QHEC existed and the polymer network was composed of QHEC chain entanglements. When introducing NaCl, the η^* of the complex solution monotonically increased, similar to Fig. 1. The screening of the electrostatic repulsion between the cationic polymeric chains led to the enhancement of the QHEC entanglements and the network density. However, a contrary η^* behavior was observed in QHEC/NCC solution with introducing NaCl, and the η^* value decreased monotonically in Fig. 7(b). The network was composed of electrostatic adsorption between QHEC and NCC as cross-linking, as well as the entanglement of the QHEC as polymer network. When adding NaCl, the electrostatic interactions between QHEC and NCC was weakened, and the QHEC entanglement was enhanced. The decreasing η^* value in Fig. 7(b) indicated the decreasing elasticity of the system, due to the reduction of the integrated interactions among the QHEC/NCC/NaCl network.

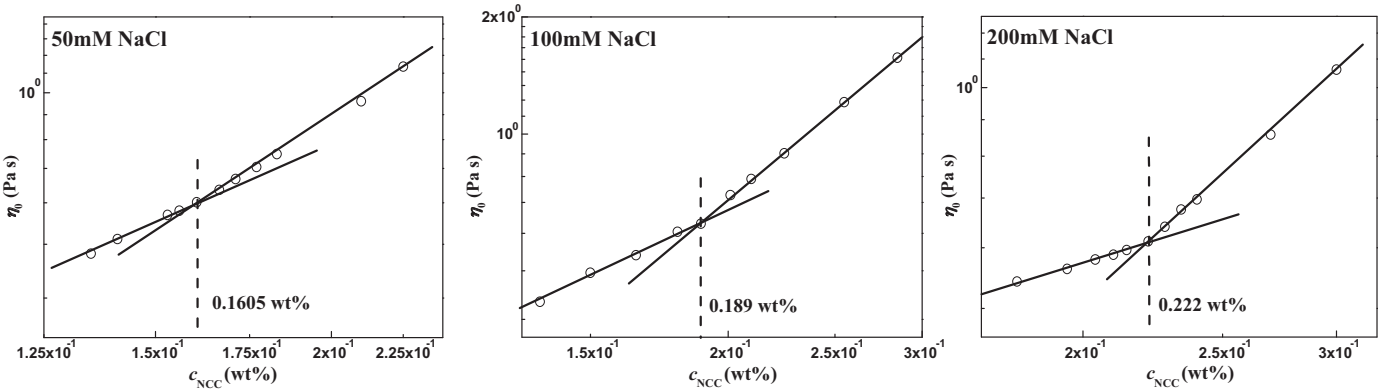

Fig. 4. η_0 as a function of c_{NCC} with 1.5 wt% QHEC in 50, 100 and 200 mM NaCl solutions.

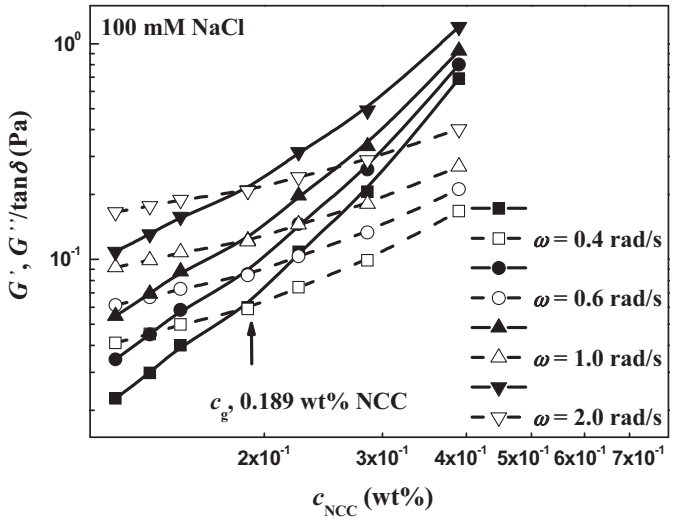

Fig. 5. Plots of G' and $G''/\tan\delta$ as a function of c_{NCC} with 1.5 wt% QHEC in 100 mM NaCl solution (ω varied from 0.4 to 2 rad s^{-1}). The arrow indicates the gel point.

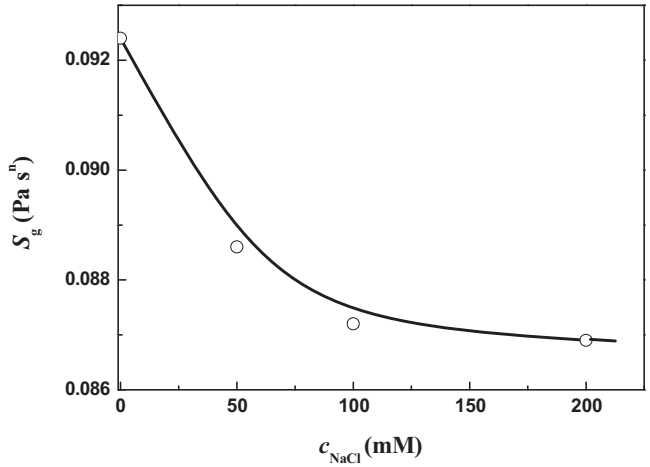

Fig. 6. S_g as a function of c_{NaCl} of the QHEC/NCC/NaCl solutions.

Therefore, the electrostatic adsorption between the QHEC and NCC exhibited more dominant contribution than the QHEC entanglements to the gel formation, which is consistent to the conclusion of Fig. 6.

Due to the critical nature of the gelation, transient rheological properties η_0 before gelation, and equilibrium modulus (G_e) beyond gelation, show a distinct scaling behavior in the vicinity of gelation (Stauffer, Coniglio, & Adam, 1982) as

$$\eta_0 \propto \varepsilon^{-\gamma} \quad \text{for} \quad p < p_g \tag{5}$$

$$G_e \propto \varepsilon^{z} \quad \text{for} \quad p > p_g \tag{6}$$

where $\varepsilon = |p_g - p|/p_g$ indicates the relative distance of a variable p departing from the gel point p_g, and p can be the cross-linking degree, gelation time, gelation temperature, gelation concentration, and so forth. γ is the critical exponent determining the critical characteristics in the vicinity of the gelation. G_e is the quasi-equilibrium modulus, and z is the scaling exponent (Ferry, 1980). The values of γ and z have been predicted by many models, and Winter et al. has proposed a scaling law to describe the relationship between n, z and γ before and beyond the gel point (Chambon & Winter, 1987; Mours & Winter, 1996; Martin, Adolf, & Wilcoxon, 1988) as

$$n = \frac{z}{(z+\gamma)} \tag{7}$$

where n is relaxation exponent, which can be calculated by Eq. (2). Since the $c_{g,NCC}$ of the QHEC/NCC/NaCl solution was obtained by Winter and Chambon theory, c_{NCC} can be used to calculate relative distance ε as

$$\varepsilon = \frac{\left|c_{g,NCC} - c_{NCC}\right|}{c_{g,NCC}} \tag{8}$$

Therefore, γ and z can be directly calculated from the slope of the plot of η_0 and G_e against ε in log–log scale.

Fig. 8(a) shows η_0 as a function of ε before gelation in the 1.5 wt% QHEC in 50, 100 and 200 mM NaCl solutions. The values from −0.084 to −0.034 represented their slopes with different c_{NaCl}. Linear fit at relatively high concentrations was obtained, as well as the discrepancy in the low concentration range. η_0 can be altered by NaCl addition, as a result of electrostatic interaction screening. However, γ was not constant, and it deceased with increasing c_{NaCl}. As shown in Eq. (7), γ is a parameter governing the gelation rate, therefore, the gelation rate was faster with lower c_{NaCl}, possibly as a result of that the electrostatic adsorption was less weakened at lower c_{NaCl}. Fig. 8(b) plotted G_e as a function of ε beyond gelation in the 1.5 wt% QHEC in 50, 100 and 200 mM NaCl

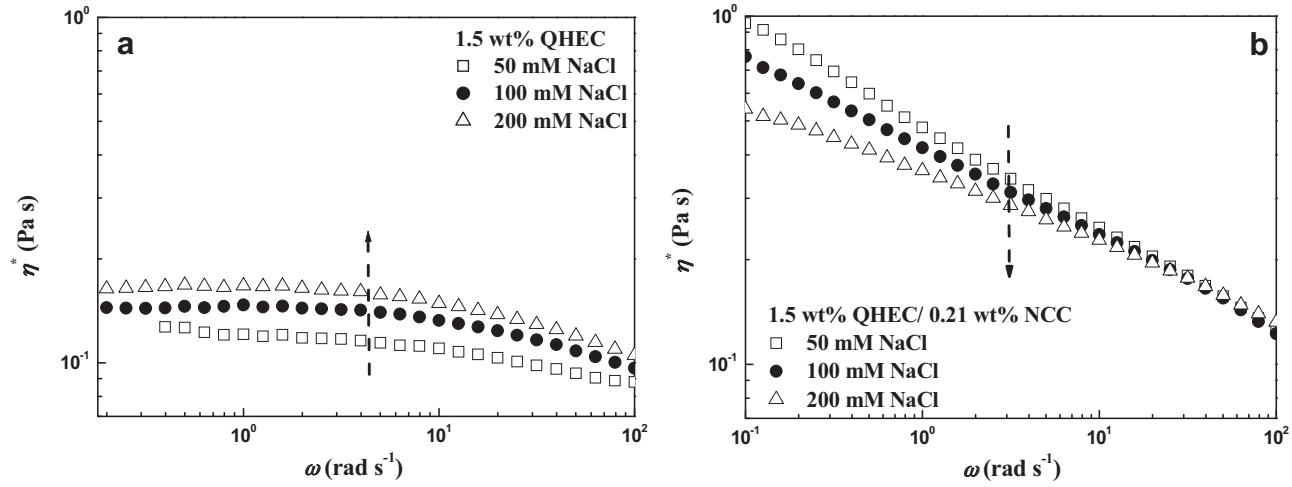

Fig. 7. η^* plots of 1.5 wt% QHEC (a) and 1.5 wt% QHEC/0.21 wt% NCC (b) in 50, 100 and 200 mM NaCl aqueous solution, respectively.

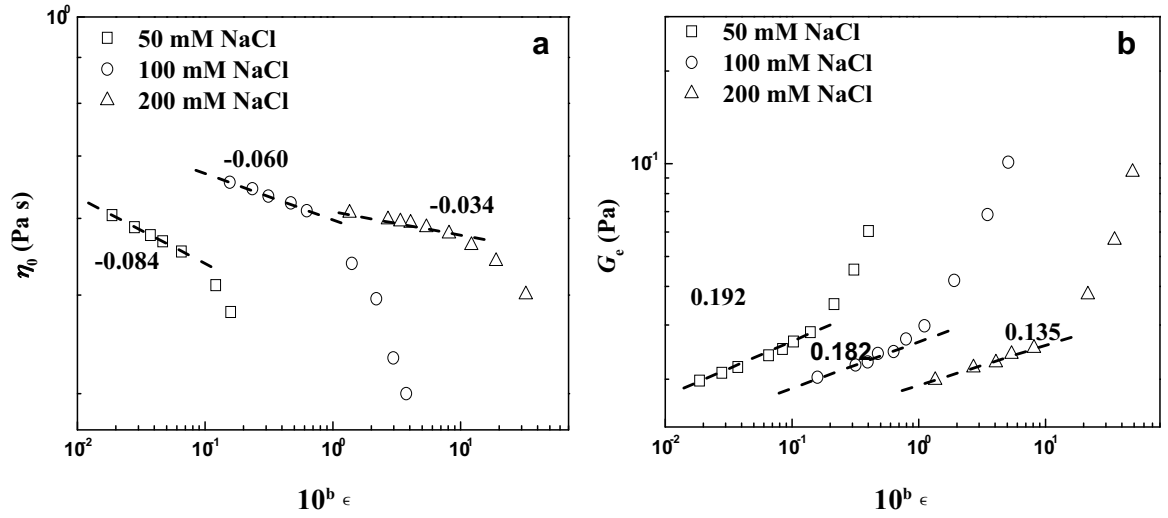

Fig. 8. η_0 (a) and G_e (b) as a function of the relative distance ε before the gel point for the 1.5 wt% QHEC in 50, 100 and 200 mM NaCl aqueous solutions, where the ε is multiplied by 10^b. The linear fittings give the solid straight lines, and the values represent the slope of the fitted lines..

solutions. The exponent z decreased with increasing c_{NaCl}, indicating the growth rates of the clusters were higher with relatively less NaCl, because the electrostatic adsorption between QHEC and NCC, which exhibited greater contribution, was less weakened.

In order to validate the applicability of scaling law as shown Eq. (7), the n values calculated by $\tan\delta$ at the gel point and scaling law, were listed in Table 1. Obviously, the scaling law was only feasible at the highest c_{NaCl} (200 mM), therefore, the scaling law was only applicable when the electrostatic interaction was completely screened. Nemoto et al. have investigated the gelation of α,ω-dihydroxyl polybutadiene/*p*-xylene system, and revealed that the intermolecular interaction, i.e., hydrogen bonding between hydroxyl groups at the chain ends in their case, has great influences on the application of scaling law, and the scaling law worked only when the hydrogen bonding interaction in the system could be neglected (Koike, Nemoto, Watanabe, & Osaki, 1996). Moreover, in the cellulose/NaOH/thiourea solution obtained at low temperature, the scaling law was not feasible at high temperatures, at which the intermolecular hydrogen bonds were re-established (Lue & Zhang, 2008), indicating the intermolecular interaction played an important role in the application of scaling law.

The plateau value of G_0 (average of $G'(\omega)$ values at the four highest angular frequencies) allows for the calculation of a network junction density ^1N via $G_0 = {}^1Nk_BT$ with ^1N the network junction density, T the temperature, and k_B the Boltzmann's constant. This in turn can be used to calculate a mesh size $d_{mesh} = 1/{}^1N(1/3)$ and then give a rough estimation for the number of NCC rods per junction $N_{agg,NCC} = {}^1N_s/{}^1N$ with the number density of NCC rods ^1N_s (Hoffmann et al., 2011). The parameters obtained from QHEC/NCC/NaCl solution at each gel point were listed in Table 2. ^1N increased as c_{NaCl} increased, indicating more junctions were needed to reach the gel point, as a result of the screening of the electrostatic interaction, and the decreasing d_{mesh} also suggested a denser network with NaCl increasing. The larger $N_{agg,NCC}$ indicated more NCC were involving in the network formation at higher c_{NaCl}, which is consistent with the result from Table 1. At the highest c_{NaCl} (200 mM) the gel network was composed of entanglements, and the inter-molecular interaction, i.e. electrostatic adsorption between QHEC and NCC, were completely screened, leading to the feasibility of scaling law, in accordance with the results of Nemoto (Koike et al., 1996). So far, the application of scaling law in a mixture system composed of oppositely charged polyelectrolyte, colloid and electrolyte has been verified, and the results suggested that the scaling low was only applicable when the inter-molecular interaction of the system was weak enough to be neglected.

In the present paper, QHEC/NCC solution with a 1.5 wt% concentration was applied, and NaCl was used to demonstrate the electrolyte influences on the gelation. In the future more QHEC concentrations and more polyelectrolyte or electrolyte with various parameters are planned to be involved, in order to give a full prospect of the phase behavior in polyeletrolyte/colloid complex solutions.

Table 2
Parameters obtained from QHEC/NCC/NaCl mixtures at the critical gel points.

Samples	^1N (m^{-3})	d_{mesh} (nm)	$N_{agg,NCC}$
50 mM NaCl	1.058×10^{21}	98	0.056
100 mM NaCl	1.098×10^{21}	96	0.063
200 mM NaCl	1.160×10^{21}	95	0.070

4. Conclusions

In the present paper, the monovalent electrolyte (NaCl) influences on the sol–gel transition and scaling law of the complex solution composed of positively charged QHEC and negatively charged NCC were investigated by rheological means. Winter and Chambon theory was proved to be applicable to describe the sol–gel transition, and the gel points were successfully determined. With increasing the c_{NaCl}, more NCC were needed to induce gelation, and larger $\tan\delta$ and relaxation exponent n values at the gel point indicated the elastic nature of mixture was weakened with NaCl introduction, consistent with the result of the S_g. The results indicated the critical network at the gel point was composed of entanglements and association of QHEC chains (as network), as well as the electrostatic adsorption interaction between QHEC and NCC (as cross-linking), among which the electrostatic adsorption played more important role than the entanglements to the gel formation. Furthermore, the exponents of scaling law $\eta_0 \propto \varepsilon^{-\gamma}$ and $G_e \propto \varepsilon^z$ of the QHEC/NCC/NaCl solution revealed that the scaling law $n = z/(z+\gamma)$ between n, γ and z was only feasible at the highest c_{NaCl}, since in that case the intermolecular interaction (electrostatic adsorption interaction in the present paper) was screened by NaCl and can be neglected, and the critical gel network was dominated by entanglements and association.

Acknowledgments

The authors thank the National Institute for Nanotechnology of National Research Council Canada for supporting this project. The work was financially supported by Alberta Innovates-BioSolutions (which includes former Alberta Forestry Research Institute) and the National Natural Science Foundation of China (51203122).

References

Allen, K. E., Murray, B. S., & Dickinson, E. (2008). Development of a model whipped cream: Effects of emulsion droplet liquid/solid character and added hydrocolloid. *Food Hydrocolloids*, *22*, 690–699.

Boluk, Y., Zhao, L., & Incani, V. (2012). Dispersions of nanocrystalline cellulose in aqueous polymer solutions: Structure formation of colloidal rods. *Langmuir*, *28*, 6114–6123.

Bondeson, D., Mathew, A., & Oksman, K. (2006). Optimization of the isolation of nanocrystals from microcrystalline cellulose by acid hydrolysis. *Cellulose*, *13*, 171–180.

Brotherson, B., Bottomley, L., Ludovice, P., & Deng, Y. (2008). Salt effect on cationic polyacrylamide conformation on mica studied by single molecule pulling with scanning probe microscopy. *The Journal of Physical Chemistry B*, *112*, 12686–12691.

Canales, M. A. M., Hidalgo, M. E., Risso, P. H., & Alvarez, E. M. (2010). Colloidal stability of bovine calcium caseinate suspensions. Effect of protein concentration and the presence of sucrose and lactose. *Journal of Chemical and Engineering Data*, *55*, 2550–2557.

Carrillo, J., & Dobrynin, A. (2011). Polyelectrolytes in salt solutions: Molecular dynamics simulations. *Macromolecules*, *44*, 5798–5816.

Chambon, F., & Winter, H. H. (1987). Linear viscoelasticity at the gel point of a crosslinking PDMS with imbalanced stoichiometry. *Journal of Rheology*, *31*, 683–697.

Chambon, F., & Winter, H. H. (1985). Stopping of crosslinking reaction in a PDMS polymer at the gel point. *Polymer Bulletin*, *13*, 499–503.

Chen, Q., Diesel, E., Whitmer, J., Bae, S., Luijten, E., & Granick, S. (2011). Triblock colloids for directed self-assembly. *Journal of the American Chemical Society*, *133*, 7725–7727.

Colby, R. H. (2010). Structure and linear viscoelasticity of flexible polymer solutions: Comparison of polyelectrolyte and neutral polymer solutions. *Rheologica Acta*, *49*, 425–442.

Dalvi, S. V., & Dave, R. N. (2009). Controlling particle size of a poorly water-soluble drug using ultrasound and stabilizers in antisolvent precipitation. *Industrial and Engineering Chemistry Research*, *48*, 7581–7593.

Dobrynin, A., & Rubinstein, M. (2005). Theory of polyelectrolytes in solutions and at surfaces. *Progress in Polymer Science*, *30*, 1049–1118.

Farrokhpay, S. (2009). A review of polymeric dispersant stabilisation of titania pigment. *Advances in Colloid and Interface Science*, *151*, 24–32.

Ferry, J. D. (1980). *Viscoelastic properties of polymers*. New York, NY: John Wiley & Sons.

Frenzel, R., Swaboda, C., Petzold, G., Emmler, R., & Simon, F. (2011). Controlling the water uptake of wood by polyelectrolyte adsorption. *Progress in Organic Coatings*, *72*, 88–95.

Gallegos, C., & Franco, J. M. (1999). Rheology of food, cosmetics and pharmaceuticals. *Current Opinion in Colloid and Interface Science*, *4*, 288–293.

Gao, S., & Nishinari, K. (2004). Effect of degree of acetylation on gelation of konjac glucomannan. *Biomacromolecules*, *5*, 175–185.

Hansson, P. (2006). Interaction between polyelectrolyte gels and surfactants of opposite charge. *Current Opinion in Colloid and Interface Science*, *11*, 351–362.

Hoffmann, I., Heunemann, P., Prévost, S., Schweins, R., Wagner, N. J., & Gradzielski, M. (2011). Self-aggregation of mixtures of oppositely charged polyelectrolytes and surfactants studied by rheology, dynamic light scattering and small-angle neutron scattering. *Langmuir*, *27*, 4386–4396.

Huang, Y., Zhou, J., Su, B., Shi, L., Wang, J., Chen, S., Wang, L., Zi, J., Song, Y., & Jiang, L. (2012). Colloidal photonic crystals with narrow stopbands assembled from low-adhesive superhydrophobic substrates. *Journal of the American Chemical Society*, *134*, 17053–17058.

Izuka, A., & Winter, H. H. (1992). Molecular weight dependence of viscoelasticity of polycaprolactone critical gels. *Macromolecules*, *25*, 2422–2428.

Junka, K., Sundman, O., Salmi, J., Österberg, M., & Laine, J. (2014). Multilayers of cellulose derivatives and chitosan on nanofibrillated cellulose. *Carbohydrate Polymers*, *108*, 34–40.

Kjøniksen, A. L., Hiorth, M., Roots, J., & Nysrtom, B. (2003). Shear-induced association and gelation of aqueous solutions of pectin. *The Journal of Physical Chemistry B*, *107*, 6324–6328.

Kjøniksen, A. L., & Nystrom, B. (1996). Effects of polymer concentration and cross-linking density on rheology of chemically cross-linked poly(vinyl alcohol) near the gelation threshold. *Macromolecules*, *29*, 5215–5222.

Kleinert, J., Kim, S., & Velev, O. (2010). Electric-field-assisted convective assembly of colloidal crystal coatings. *Langmuir*, *26*, 10380–10385.

Koike, A., Nemoto, N., Watanabe, Y., & Osaki, K. (1996). Dynamic viscoelasticity and FT-IR measurements of end-crosslinking α,ω-dihydroxyl polybutadiene solutions near the gel point in the gelation process. *Polymer Journal*, *28*, 942–950.

Kumar, A., Dubin, P. L., Hernon, M. J., Li, Y., & Jaeger, W. (2007). Ag/polypyrrole core–shell nanostructures: Interface polymerization, characterization, and modification by gold nanoparticles. *The Journal of Physical Chemistry B*, *111*, 8468–8476.

Larson, R. G. (1999). *The structure and rheology of complex fluids*. Oxford University Press: New York, NY.

Lee, S. Y., Gradon, L., Janeczko, S., Iskandar, F., & Okuyama, K. (2010). Formation of highly ordered nanostructures by drying micrometer colloidal droplets. *ACS Nano*, *4*, 4717–4724.

Lee, W., Chan, A., Bevan, M. A., Lewis, J. A., & Braun, P. V. (2004). Nanoparticle-mediated epitaxial assembly of colloidal crystals on patterned substrates. *Langmuir*, *20*, 5262–5270.

Leunissen, M., Christova, C., Hynninen, A. P., Royall, C., Campbell, A., Imhof, A., Dijkstra, M., Roij, R., & van Blaaderen, A. (2005). Ionic colloidal crystals of oppositely charged particles. *Nature*, *437*, 235–240.

Li, L., Uchida, H., & Aoki, Y. (1997). Rheological images of poly(vinyl chloride) gels. 2. Divergence of viscosity and the scaling law before the sol–gel transition. *Macromolecules*, *30*, 7842–7848.

Liu, D., Chen, X., Yue, Y., Chen, M., & Wu, Q. (2011). Structure and rheology of nanocrystalline cellulose. *Carbohydrate Polymers*, *84*, 316–322.

Liu, D., Zhong, T., Chang, P., Li, K., & Wu, Q. (2010). Starch composites reinforced by bamboo cellulosic crystals. *Bioresource Technology*, *101*, 2529–2536.

Liu, D., Li, J., Sun, F., Xiao, R., Guo, Y., & Song, J. (2014). Liquid crystal microphase separation of cellulose nanocrystals in the wet-spun PVA composite fibers. *RSC Advances*, http://dx.doi.org/10.1039/C4RA04063E

Lu, A., Hemraz, U., Khalili, Z., & Boluk, Y. (2014). Unique viscoelastic behaviors of colloidal nanocrystalline cellulose aqueous suspensions. *Cellulose*, *21*, 1239–1250.

Lu, A., Wang, Y., & Boluk, Y. (2014). Investigation of the scaling law on gelation of oppositely charged nanocrystalline cellulose and polyelectrolyte. *Carbohydrate Polymers*, *105*, 214–221.

Lue, A., & Zhang, L. (2008). Investigation of the scaling law on cellulose solution prepared at low temperature. *The Journal of Physical Chemistry B*, *112*, 4488–4495.

Madbouly, S. A., Xia, Y., & Kessler, M. R. (2012). Rheokinetics of ring-opening metathesis polymerization of bio-based castor oil thermoset. *Macromolecules*, *45*, 7729–7739.

Martin, J. E., Adolf, D., & Wilcoxon, J. P. (1988). Viscoelasticity of near-critical gels. *Physical Review Letters*, *61*, 2620–2623.

Martinez, C. J., Liu, J., Rhodes, S. K., Luijten, E., Weeks, E. R., & Lewis, J. A. (2005). Interparticle interactions and direct imaging of colloidal phases assembled from microsphere–nanoparticle mixtures. *Langmuir*, *21*, 9978–9989.

McGrath, J., Bock, R., Cathcart, J. M., & Lyon, L. A. (2007). Self-assembly of paint-on colloidal crystals using poly(styrene-*co*-*N*-isopropylacrylamide) spheres. *Chemistry of Materials*, *19*, 1584–1591.

Mours, M., & Winter, H. H. (1996). Relaxation patterns of nearly critical gels. *Macromolecules*, *29*, 7221–7229.

Nijenhuis, K., & Winter, H. H. (1989). Mechanical properties at the gel point of a crystallizing poly(vinyl chloride) solution. *Macromolecules*, *22*, 411–414.

Nordby, M. H., Kjøniksen, A. L., Nyström, B., & Roots, J. (2003). Thermoreversible gelation of aqueous mixtures of pectin and chitosan. Rheology. *Biomacromolecules*, *4*, 337–343.

Pantina, P., & Furst, E. (2004). Directed assembly and rupture mechanics of colloidal aggregates. *Langmuir*, *20*, 3940–3946.

Pickrahn, K., Rajaram, B., & Mohraz, A. (2010). Relationship between microstructure, dynamics, and rheology in polymer-bridging colloidal gels. *Langmuir*, *26*, 2392–2400.

Qi, A., Chan, P., Ho, J., Rajapaksa, A., Friend, J., & Yeo, L. (2011). Template-free synthesis and encapsulation technique for layer-by-layer polymer nanocarrier fabrication. *ACS Nano*, *5*, 9583–9591.

Regismond, S. T. A., Heng, Y. M., Goddard, E. D., & Winnik, F. M. (1999). Fluorescence microscopy observation of the adsorption onto hair of a fluorescently labeled cationic cellulose ether. *Langmuir*, *15*, 3007–3010.

Russel, W. B., Saville, D. A., & Schowalter, W. R. (1989). *Colloidal dispersions*. Cambridge University Press: New York, NY.

Sabourin, J., Dabbs, D., Yetter, R., Dryer, F., & Aksay, I. (2009). Functionalized graphene sheet colloids for enhanced fuel/propellant combustion. *ACS Nano*, *3*, 3945–3954.

Shi, X., Lu, A., Cai, J., Zhang, L., Zhang, H., Li, J., & Wang, X. (2012). Rheological behaviors and miscibility of mixture solution of polyaniline and cellulose dissolved in an aqueous system. *Biomacromolecules*, *13*, 2370–2378.

Sivakumar, S., Bansal, V., Cortez, C., Chong, S., Zelikin, A. N., & Caruso, F. (2009). Degradable, surfactant-free, monodisperse polymer-encapsulated emulsions as anticancer drug carriers. *Advanced Materials*, *21*, 1820–1824.

Song, H., Niu, Y., Wang, Z., & Zhang, J. (2011). Liquid crystalline phase and gel – sol transitions for concentrated microcrystalline cellulose (mcc)/1-ethyl-3-methylimidazolium acetate (EMIMAc) solutions. *Biomacromolecules*, *12*, 1087–1096.

Stauffer, D., Coniglio, A., & Adam, A. (1982). Gelation and critical phenomena. *Advances in Polymer Science*, *44*, 103–158.

Tung, C. Y. M., & Dynes, P. J. (1982). Relationship between viscoelastic properties and gelation in thermosetting systems. *Journal of Applied Polymer Science*, *27*, 569–574.

Wang, Y., Lue, A., & Zhang, L. (2009). Rheological behavior of waterborne polyurethane/starch aqueous dispersions during cure. *Polymer*, *50*, 5474–5481.

Wang, H., & Roman, M. (2011a). Formation and properties of chitosan–cellulose nanocrystal polyelectrolyte–macroion complexes for drug delivery applications. *Biomacromolecules*, *12*, 1585–1593.

Wang, H., & Roman, M. (2011b). Effects of pH and salt concentration on the formation and properties of chitosan–cellulose nanocrystal polyelectrolyte–macroion complexes. *Biomacromolecules*, *12*, 3708–3714.

Whitmer, J., & Luijten, E. (2011). Influence of hydrodynamics on cluster formation in colloid polymer mixtures. *Journal of Physical Chemistry B*, *115*, 7294–7300.

Winter, H. H., & Chambon, F. (1986). Analysis of linear viscoelasticity of a crosslinking polymer at the gel point. *Journal of Rheology*, *30*, 367–382.

Yap, H. P., Quinn, J. F., Ng, S. M., Cho, J., & Caruso, F. (2005). Colloid surface engineering via deposition of multilayered thin films from polyelectrolyte blend solutions. *Langmuir*, *21*, 4328–4333.

Ye, X., Tong, P., & Fetters, L. J. (1997). Neutron scattering study of colloidal interactions in an adsorbing polymer solution. *Macromolecules*, *30*, 4103–4111.

Zuzzi, S., Cametti, C., Onori, G., Sennato, S., & Tacchi, S. (2009). Polyion-induced cluster formation in different colloidal polyparticle aqueous suspensions. *Langmuir*, *25*, 5910–5917.